Modelling Tsunami Generated by Submarine Landslides

R.I. Nokes[1], L.P. Sue[2] and M.J. Davidson[1]

[1]Department of Civil and Natural Resources Engineering
University of Canterbury, Christchurch 8140, New Zealand

[2] Beca Pty Ltd
Melbourne, Victoria, Australia

Abstract

A variety of physical processes associated with the generation of tsunamis by two-dimensional submarine landslides in a uniform depth fluid are explored with a semi-analytical model based on linear, inviscid, irrotational wave theory. The results demonstrate that the maximum potential energy in the wave field is approximately linearly proportional to the initial acceleration of the landslide and inversely proportional to the relative water depth, provided the initial acceleration is more than an order of magnitude smaller than the gravitational acceleration. It is shown that when the landslide is moving at a constant velocity, or Froude number, energy can be gained by, or lost from, the wave field through ongoing interaction with the landslide motion.

1. Introduction

Tsunamis, generated by the collapse of continental shelf sediments, can cause significant damage to coastal infrastructure [1-3]. A particular hazard associated with these submarine landslide generated tsunamis is the very short timescale between the causation event and the impingement of the waves on the shoreline.

Considerable research has been undertaken in the last 50 years to better understand the manner in which these tsunamis are generated. This work has been field based, experimental and theoretical/computational in nature (see Sue et al [4] and the references therein).

Many of these studies have considered the practical problem of a 2D or 3D landslide moving down a sloping boundary and the focus has been on the calibration of numerical models against experimental data. In this paper we consider an idealised problem where the landslide motion is along a horizontal boundary. This geometry enables us to employ a semi-analytical model that is computationally efficient and which provides clearer insights into the mechanisms by which energy is transferred from the landslide motion to the wave field and in particular it enables a clear picture of the onshore propagating wave field to be obtained. While this geometry is physically unrealistic most continental shelves have fairly shallow slopes and the proposed model could be seen to have predictive capability in a local sense.

2. Mathematical model

The physical problem to be explored is illustrated in figure 1. A low aspect rigid landslide moves along the bottom boundary of a water body of uniform depth, D.

The model presented here is based on the assumption that the flow is two-dimensional, inviscid and irrotational. We will assume that the linear assumption is valid for free surface disturbances, and that the low aspect ratio of the moving landslide allows a similar approximation to be invoked on the bottom boundary. This will allow a semi-analytical technique to be employed to solve the governing equations. Based on these assumptions the governing equations are

$$\nabla^2 \phi = 0 \tag{1}$$

$$-\frac{\partial \phi}{\partial n} = v_{nb} \quad \text{on} \quad y = y_b(x,t) \tag{2}$$

$$\frac{\partial \eta}{\partial t} = \frac{\partial \phi}{\partial y} \quad \text{on} \quad y = 0 \tag{3}$$

$$\frac{\partial \phi}{\partial t} + g\eta = 0 \quad \text{on} \quad y = 0 \tag{4}$$

$$\phi(x,y,0) = 0 \quad \eta(x,0) = 0 \tag{5}$$

The function $y_b(x,t)$ specifies the shape of the bottom boundary, which includes the time-dependent moving landslide, and encapsulates the forcing for the problem; n is an outward normal to this boundary and v_{nb} is its normal velocity. The linear assumption has been invoked for the free surface boundary conditions.

We choose suitable non-dimensional variables based on the length of the landslide and its initial acceleration a_0 (discussed in the next section). These are

$$x' = \frac{x}{L_b} \;,\; y' = \frac{y}{L_b} \;,\; \eta' = \frac{\eta}{L_b} \;,$$

$$\phi' = \frac{\phi}{\sqrt{a_0 L_b{}^3}} \;,\; t' = t\sqrt{\frac{a_0}{L_b}} \tag{6}$$

By invoking the linear assumption for the bottom boundary condition so that the boundary condition is imposed on the horizontal boundary, these transformations yield

$$\nabla^2 \phi = 0 \tag{7}$$

$$-\frac{\partial \phi}{\partial y} = v_{nb} \quad \text{on} \quad y = -\tau \tag{8}$$
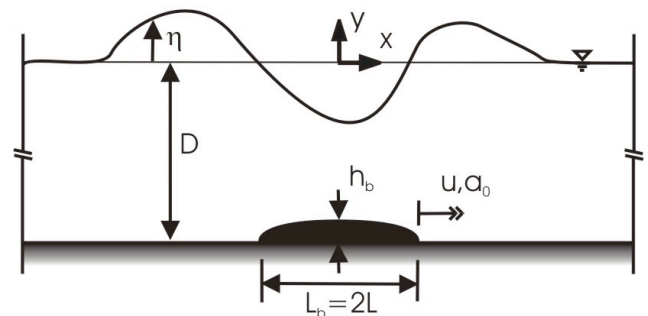

Figure 1. The flow domain and the definition of the key variables.

$$\frac{\partial \eta}{\partial t} = \frac{\partial \phi}{\partial y} \quad \text{on} \quad y = 0 \tag{9}$$

$$\lambda \frac{\partial \phi}{\partial t} + \eta = 0 \quad \text{on} \quad y = 0 \tag{10}$$

$$\phi(x, y, 0) = 0 \quad \eta(x, 0) = 0 \tag{11}$$

In equations (7)-(11) the primes have been dropped for clarity. This non-dimensionalisation process has generated two important dimensionless parameters that play a key role in the physics of the problem. They are

$$\lambda = \frac{a_0}{g}, \quad \text{and} \quad \tau = \frac{D}{L_b} \tag{12}$$

the dimensionless initial acceleration and the ratio of water depth to landslide length respectively.

The bottom boundary position, including the landslide, can be written in dimensionless form as

$$y_b(t) = -\tau + \xi f(u(t)) \tag{13}$$

where $u(t)$ can be thought of as a dimensionless local landslide coordinate measured from the position of its centre of mass, $x_0(t)$, and is defined as

$$u(t) = x - x_0(t) \tag{14}$$

$f(u)$ is a landslide shape function, and ξ is the landslide aspect ratio given by

$$\xi = \frac{h_b}{L_b} \tag{15}$$

Thus the normal velocity imposed on the bottom boundary is

$$v_{nb} = \xi \frac{\partial f}{\partial t} = -\xi \frac{df}{du} \frac{dx_0}{dt} \tag{16}$$

2.1 Landslide motion

In order to keep the problem tractable the motion of the slider centre of mass, $x_0(t)$, is constrained in the following way. At $t = 0$ the landslide motion begins with a constant acceleration. At some later time, t_{max}, the landslide ceases to accelerate and either continues at a constant velocity or begins to decelerate, again at a constant rate. In the former case the landslide may begin to slow, at a constant deceleration, at a later time denoted t_{dec}. If the landslide does decelerate it comes to a halt at $t = t_{zero}$.

2.2 Spectral solution technique

The solution method for this problem is based on a spectral decomposition of the various flow fields (see Lighthill [5]). The modes in this decomposition can be written in dimensionless form as

$$e^{i\left(kx - \frac{wt}{\sqrt{\lambda}}\right)} = e^{i\sigma} \tag{17}$$

where the non-dimensional wavenumber and frequency are given by

$$k' = kL_b, \quad \text{and} \quad \omega' = \omega \sqrt{\frac{L_b}{g}} \tag{18}$$

Solutions for the velocity potential and free surface elevation are assumed to be of the forms

$$\phi = \int_{-\infty}^{\infty} e^{i\sigma} \left[a(k,t) \cosh k(y+\tau) + b(k,t) \sinh k(y+\tau) \right] dk \tag{19}$$

and

$$\eta(x,t) = \int_{-\infty}^{\infty} c(k,t) e^{i\sigma} dk \tag{20}$$

The coefficients $a(k,t)$, $b(k,t)$, and $c(k,t)$ are complex and only the real parts of the equations (19) and (20) are required. The bottom boundary condition can also be decomposed in the same fashion. Thus we define

$$\frac{df}{du} = \int_{-\infty}^{\infty} p(k) e^{iku} dk \tag{21}$$

By applying the three boundary conditions and utilising the requirement that each of the Fourier modes is independent, equations can be obtained for the three sets of coefficients. As the free surface response is our primary focus only the equation for $c(k,t)$ is given. This is

$$\frac{d^2 c}{dt^2} - \frac{2i\omega}{\sqrt{\lambda}} \frac{dc}{dt} = F(k,t) \tag{22}$$

where the forcing function $F(k,t)$ is defined to be

$$F(k,t) = \frac{\xi e^{i\theta} p(k)}{\cosh(k\tau)} \left(ik \left(\frac{dx_0}{dt} \right)^2 - \frac{d^2 x_0}{dt^2} \right) \tag{23}$$

and

$$\theta(k,t) = \frac{\omega t}{\sqrt{\lambda}} - kx_0(t) \tag{24}$$

Note that k is treated as a parameter in equation (22), hence the use of ordinary derivatives.

Analytical solutions to equation (22) are not readily available so a numerical integration technique was employed. This technique involved the following steps:

1. A range of wavenumbers to be used in the integral in equation (20) was selected. k_{max} determined the smallest length scale resolved.
2. An appropriate discretisation of the wave number space was selected. The spacing, Δk, determined the largest scale resolved by the model and hence determined the space scale over which the solution repeated.
3. A 4th order Runge-Kutta scheme was used to integrate equation (22) for each value of k.
4. Equation (20) was integrated numerically to provide $\eta(x,t)$.

While a full analytical solution was not possible the numerical integration of equation (22) was computationally substantially more efficient than a full numerical solution using the boundary element method. In addition, while not described here, this spectral solution enabled the wave field to be separated into forward and backward propagating wave components, as illustrated in Figures 4 and 5.

3. Results

3.1 Dependence on landslide shape

The dependence of the wave field on the shape of the landslide was first explored. Four separate shapes, all symmetrical about the centre of the landslide, were incorporated into the forcing function $F(x,t)$ – a sawooth, a half cosine, a half cosine squared and a quartic. Figure 2 shows that the wave fields generated for the various shapes became indistinguishable when the volume of fluid displaced by the landslide was the same – a result with important practical implications. For the remainder of this study a landslide in the shape of a sawtooth was used.
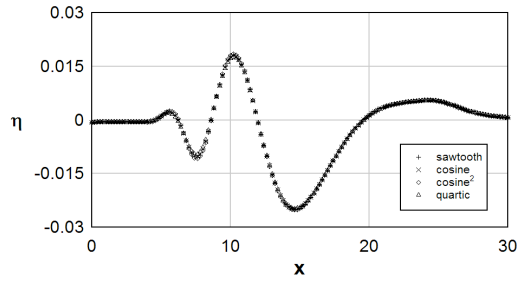
Figure 2. The wave fields generated by the four different landslide shapes for a landslide undergoing constant acceleration. t = 3.53, τ = 1, λ = 0.152 and ξ = 0.1. The volumes of the landslides were the same.
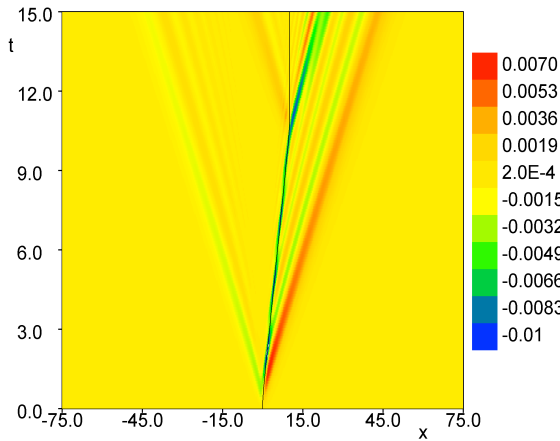

Figure 3. Wave field generated by a landslide undergoing a constant acceleration until t = 1, a constant velocity until t = 10 and then a deceleration until t = 11. The model parameters are τ = 1, λ = 0.1 and ξ = 0.1. The colour indicates the free surface amplitude. The fine solid black line corresponds to the track of the landslide.

3.2 General observations

Figure 3 presents the wave field generated by a landslide suffering an initial acceleration, followed by a period of constant velocity and finally a deceleration before coming to rest. In this case the constant velocity regime corresponded to a landslide Froude number, based on the landslide speed and the speed of a long wave, that was sub-critical. The key characteristics of such wave fields are illustrated. The initial acceleration causes a free wave, in the form of a crest to propagate ahead of the landslide, while a smaller amplitude trough propagates in the opposite direction. Above the landslide, while it is in motion, a trough is trapped (as would be found in a steady open channel flow at sub-critical Froude number). Due to the dispersive nature of the waves the energy in the forward and backward propagating wave packets gradually spreads and additional crests and troughs are created at the rear of these packets. For the rightward propagating wave packet these waves propagate past, and away from, the landslide. Once the landslide halts the trapped trough is free to propagate, and the deceleration of the landslide generates two new wave packets one travelling forward and one backward. The backward propagating packet is distinguished by a leading crest caused by the deceleration of the landslide.

Figures 4 and 5 provide spatial surface profiles, at t = 6 and t = 13, for the same simulation as that illustrated in figure 3. The two propagating wave packets (identified on either side of x = 0) are clearly seen in figure 4. An interesting feature of the wave field, while the landslide is still in motion, is the non-zero mass and momentum fluxes within each of the two wave packets. The right propagating packet is transporting positive mass in the positive x direction, while the left propagating waves are carrying a

negative mass (relative to the undisturbed free surface) in that direction. This result is perhaps unexpected for a solution obtained from linear wave theory, and is more consistent with the non-linear theory required to generate solitary waves. It is our hope to characterise and quantify these fluxes in future research. Figure 5 presents the free surface profile after the landslide has stopped. The deceleration of the landslide has rebalanced the mass and momentum fluxes by sending a positive mass pulse travelling in the negative x direction (as seen just to the right of the origin). Now both wave packets possess zero mass and momentum fluxes.
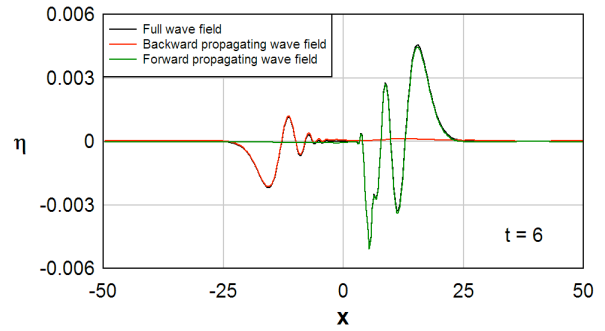

Figure 4. Wave field at t = 6 for the simulation described in Fig 3. The landslide is at x = 5.5, coinciding with the position of the largest trough – the trapped wave. The method by which the backward and forward propagating wave fields are obtained are not discussed in the present paper.
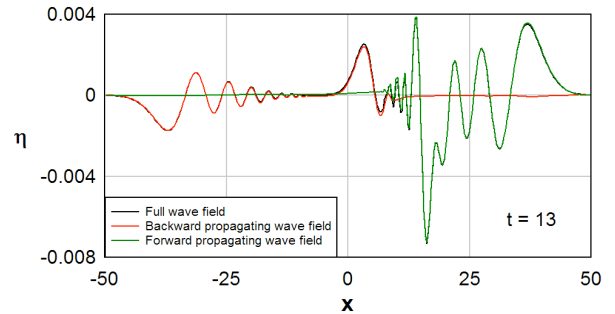

Figure 5. Wave field at t = 13 for the simulation described in Fig 3. The landslide is stationary at x = 10.

3.3 λ and τ dependence

Clearly two of the most important parameters governing the free surface response to the motion of the submarine landslide are the dimensionless initial acceleration, λ, and the dimensionless depth, τ. One measure of the intensity of the waves generated by the subsurface motion is the total potential energy possessed by the wave field. Figure 6 presents the dimensionless wave potential energy as a function of dimensionless depth, for a variety of initial accelerations. The simulations reported in this figure all included a period of constant acceleration, followed by a period of constant velocity, and finally a period of constant deceleration. To be able to compare the results in a meaningful way the Froude number of the landslide during the constant velocity phase was 0.25 in all simulations. In addition the magnitude of the deceleration matched that of the acceleration.

The maximum potential energy is multiplied by τ in figure 6. Over the majority of the depth range the scaled potential energy is effectively constant for each of the acceleration values. As the acceleration increases in magnitude the range over which the scaled potential energy is constant decreases and the scaled energy drops substantially for small depth ratios.

The figure also demonstrates that, while increasing the initial acceleration increases the potential energy contained in the wave field for small values of initial acceleration, this trend does not continue to high accelerations, as illustrated by the small increase in potential energy when the initial acceleration is doubled from 0.2 to 0.4. In practice landslide accelerations are likely to be considerably less than the gravitational acceleration and thus the almost linear dependencies on λ and $1/\tau$ are likely to be relevant for field applications.

As explained in the next section the energy content in the wave field is strongly dependent on the Froude number of the landslide in the constant velocity phase.
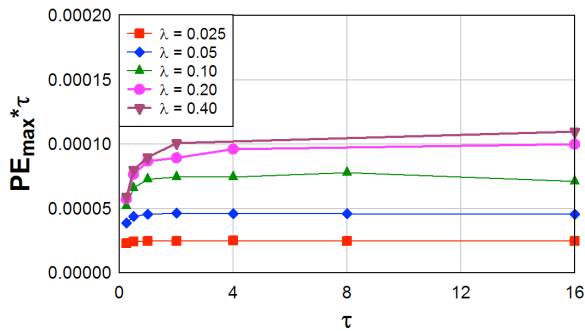

Figure 6. The dependence of the dimensionless wave potential energy on the two model parameters, the dimensionless acceleration, λ, and the dimensionless depth, τ.

3.4 Wavefield–landslide interaction

The Proudman resonance [6] is a well understood phenomenon that occurs when a travelling atmospheric pressure disturbance propagates at the same speed as a long wave on the fluid body over which it moves. Because of the locking of the forcing to the wave the pressure field has the ability to continually pump energy into the wave field, yielding large amplitude waves. The pressure field surrounding a moving submarine landslide can perform a similar action on the wave field above. Figure 7 illustrates this effect for a landslide again undergoing a constant acceleration, followed by a constant velocity phase and ultimately a constant deceleration. The landslide Fr during the constant velocity phase was varied. The maximum potential energy of the wave field is plotted as a function of landslide Fr. The maximum potential energy divided by the Fr^2 is also plotted. This normalisation is intended to reference the wave potential energy to the maximum landslide kinetic energy. A resonance peak near Fr = 1 is clear in the potential energy plot, although this peak shifts to slightly lower Fr in the normalised case.
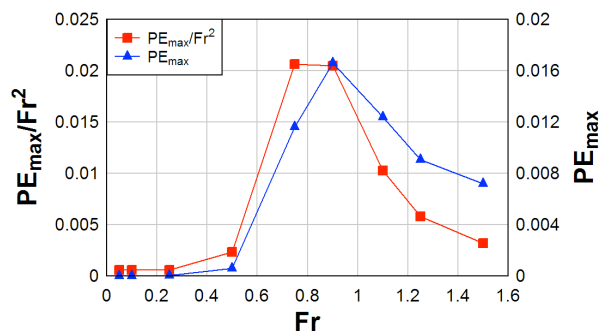

Figure 7. The dependence of the maximum dimensionless wave potential energy on the landslide Froude number for a simulation with λ=0.1, and τ=2.

This resonance phenomenon is associated with ongoing interactions between the forcing, the pressure field surrounding the landslide, and the wave field. This interaction is always present and produces interesting effects when the landslide is moving at a constant velocity for a significant period. For a sub-critical landslide Fr the crests and troughs in the dispersed wave field continually overtake the landslide as illustrated in figure 3. When a crest passes over a low pressure region, such as that above the moving landslide, the pressure field does negative work on the wave field and the PE decreases. The opposite effect occurs when a trough passes over a low pressure region. This effect is illustrated in figure 8. Here the wave potential energy is plotted against time for a landslide that has accelerated to a constant velocity at t = 5 and remained at a constant Fr of 0.25 thereafter. The significant energy exchanges between landslide and wave field are clear from the oscillations present after t = 5.
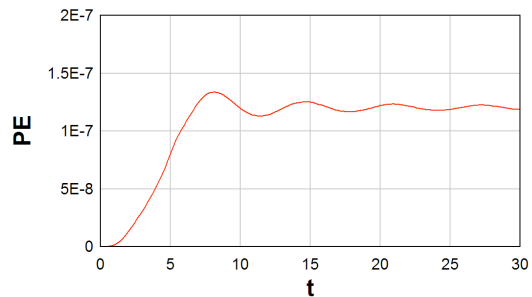

Figure 8. The time varying wave potential energy of a landslide that undergoes a constant acceleration (λ= 0.05) until t = 5. Subsequently the landslide velocity and Froude number are constant. Fr = 0.25, and τ=4.

4. Conclusions

A computationally efficient mathematical model of tsunami generated by submarine landslides along a horizontal bottom, based on a spectral decomposition of the wave field and forcing, has been presented. The results demonstrate that the conversion of landslide kinetic energy to wave field potential energy is strongly dependent on the initial acceleration of the landslide, the relative depth of the fluid layer and the Froude number of the landslide. Complex interactions between the wave field and landslide have been shown to have the potential to cause energy transfer both into, and out of, the wave field.

References

[1] Lynett, P., Borrero, J., Liu, P., & Synolakis, C., Field survey and numerical simulations: A review of the 1998 papua new guinea tsunami. *Pure and Applied Geophysics* **160** (10-11), 2003, 2119-2146.

[2] Fine, I., Rabinovich, A., Bornhold, B., Thomson, R., & Kulikov, E., The grand banks landslide-generated tsunami of november 18, 1929: Preliminary analysis and numerical modeling. *Marine Geology* **215** (1-2 SPEC ISS), 2005, 45-57.

[3] Synolakis, C., Bardet, J-P., Borrero, J., Davies, H., Okal, E., Silver, E., Sweet, S., & Tappin, D., The slump origin of the 1998 papua new guinea tsunami. *Proc R Soc London A* **458**, 2002, 763-789.

[4] Sue, L., Nokes, R., & Davidson, M., Tsunami generation by submarine landslides: Comparison of physical and numerical models, Submitted to *Env. Fluid Mech*. 2010.

[5] Lighthill, J., *Waves in Fluids*, Cambridge University Press, 1980.

[6] Proudman, J., The effects on the sea of changes in atmospheric pressure. *Geophysical Supplement to the Monthly Notices of the Royal Astronomical Society* **2** (4) 1929, 197–209